# Solid-State Study of Charge-Transfer Interactions in Copolymers

**Alexandra Simmons and Almeria Natansohn***

*Department of Chemistry, Queen's University, Kingston, Ontario, Canada K7L 3N6*

*Received March 7, 1990; Revised Manuscript Received May 15, 1990*

ABSTRACT: Random copolymers of (*N*-ethylcarbazol-3-yl)methyl methacrylate (NECMM), an electron donor, with 2-[(3,5-dinitrobenzoyl)oxy]ethyl methacrylate (DNBEM), an electron acceptor, were prepared by free-radical copolymerization. Homo- and copolymers containing from 0 to 100 mol % NECMM were made and subjected to different processing regimes. Reactivity ratios in toluene were 0.80 for NECMM and 0.81 for DNBEM. The copolymer $T_g$ values obtained by DSC show a strong positive deviation from the weighted average of the homopolymers and were fitted by the Kwei expression with $q = 69.4$, a reflection of strong interactions between donor and acceptor repeat units. Proton rotating-frame spin–lattice relaxation time constants, $T_{1\rho}$ ($^1$H), were obtained by using CP/MAS $^{13}$C solid-state NMR. The $T_{1\rho}$ values show a negative deviation from the weighted average of the homopolymers, indicating more efficient spin diffusion in the copolymers due to the charge-transfer interactions. Solid-state NMR shows residual THF is strongly bound in some samples, it is able to relax nearby protons, resulting in the observation of two $T_{1\rho}$s for different regions in the same molecule.

## Introduction

Specific interactions play a primary role in determining polymer–polymer compatibility and the physical properties of polymer blends. Knowledge about the nature and effect of different types of interactions is essential for continued progress in the development of these important materials. Charge-transfer interactions are of interest not only because they can be used to influence the morphology of polymer blend systems[1] but also because their strength is believed to be related to photoconductivity, especially with respect to visible light.[2] The main goal of ongoing studies in our laboratory is to achieve a sufficient understanding of charge-transfer interactions in polymers. This would give us the ability to design macromolecules such that their desirable properties are maximized. A more fundamental interest is the elucidation of the importance of charge-transfer interactions as one of the types of nonbonding interactions responsible for the self-organization of polymer systems.

The donor and acceptor monomers selected for use in the present study are (*N*-ethylcarbazol-3-yl)methyl methacrylate (NECMM) and 2-[(3,5-dinitrobenzoyl)oxy]-ethyl methacrylate (DNBEM). Percec et al.[3] prepared blends of the donor and acceptor homopolymers and characterized them with differential scanning calorimetry (DSC). They found pNECMM and pDNBEM to be miscible in all proportions, but phase separation occurred upon heating above 185 °C, which was attributed to decomplexation. In these blends only intermolecular interactions are possible. However, in NECMM-*co*-DNBEM copolymers, both inter- and intramolecular interactions are present. Therefore, the donor–acceptor copolymers were prepared, and the investigation of the charge-transfer interactions by DSC and solid-state NMR is described here.

Polymeric charge-transfer complexes have already been investigated by NMR spectroscopy in solution. Chemical shifts are sensitive to changes in electron density, and one would expect the electron donor resonances to be shifted downfield due to deshielding and the acceptor resonances to move upfield. In fact, $^{13}$C NMR has revealed that all shifts are in the upfield direction, due to the aromatic shielding ensuing upon the formation of stacks of interacting groups.[4]

Nearly all polymers find their application in the solid state. In addition, solvent surely influences the charge-transfer interactions. Therefore, it is necessary to carry out solid-state NMR investigations on such systems, in spite of the added complications. Cross-polarization (CP) and magic angle spinning (MAS) now make it possible to obtain high-resolution NMR spectra of bulk polymers. A previous paper describes effects on the chemical shifts in CP/MAS $^{13}$C spectra of NECMM/DNBEM copolymers and homopolymer blends, which parallel those observed in solution.[5]

Another way in which solid-state NMR can yield unique information about interactions in bulk polymers is through the observation of relaxation behavior. The relaxation behavior is sensitive to changes in mobility brought about by the interactions and can also be used to determine the homogeneity of polymer blends. Spin diffusion, in particular, is an excellent probe for mixing on the molecular level, due to its strong dependence on internuclear distance.[6] The maximum diffusive path length, and therefore minimum size of heterogeneities, that can be detected is of the order of a nanometer.[7] In fact, proton spin diffusion has proven useful in the study of blend morphology.[6,8,19]

For this paper, we chose to observe proton spin–lattice relaxation time constants in the rotating frame ($T_{1\rho}(^1H)$), which reflect the efficiency of spin diffusion. The sensitivity of rotating-frame experiments to magnetic fluctuations due to motions in the kilohertz range makes the results more directly comparable to dynamic mechanical and thermal data than laboratory-frame experiments, which detect motion in the fast megahertz range.[7] Spin diffusion is also being used to study blends of pNECMM with pDNBEM before and after decomplexation, and the results will be the subject of another report.

## Experimental Section

The synthesis of the donor and acceptor monomers is described elsewhere. In summary, NECMM is produced by the reduction of (*N*-ethylcarbazol-3-yl)carboxaldehyde to (*N*-ethylcarbazol-3-yl)methanol, followed by reaction with methacryloyl chloride.[9] Addition of ethylene glycol to 3,5-dinitrobenzoic acid yields 2-[(3,5-dinitrobenzoyl)oxy]ethanol, which is similarly reacted with methacryloyl chloride to give DNBEM, the acceptor monomer.[10]

Homo- and copolymers were produced by free-radical polymerization of 0.5 M solutions of the monomers in toluene at 60 °C for 4 days, in the presence of AIBN at a level of 1% on the weight of monomer. Polymers were isolated by two reprecipitations from THF into methanol and dried for several days

0024-9297/90/2223-5127$02.50/0 © 1990 American Chemical Society

**Table I**
**$T_g$ Values for NECMM-*co*-DNBEM from DSC**

| NECMM in copolymer, mol % | $T_g$, °C | | |
|---|---|---|---|
| | precipitd | evapd (THF) dried 60 °C | evapd (THF) dried above $T_g$ |
| 0 | 99 | | |
| 13.5 | 111 | | |
| 27.4 | 122 | 111 | 121 |
| 37.1 | 130 | 122 | 127 |
| 49.5 | 135 | 128 | 134 |
| 62.5 | 141 | 124 | 136 |
| 73.6 | 142 | 130 | 142 |
| 87.3 | 141 | | |
| 100.0 | 139 | | |

under vacuum at 60 °C. One set of samples was then redissolved in boiling THF at a concentration of 2.5% w/v and cooled, and the THF allowed to evaporate slowly, followed by drying either at 60 °C or above the polymer's $T_g$, under vacuum.

The composition of the polymers was obtained by $^1$H NMR spectroscopy in $CDCl_3$/DMSO-$d_6$ 50/50 v/v at 100 °C to ensure complete dissolution and sufficient spectral resolution.

Polymer glass transition temperatures were determined by differential scanning calorimetry by using a Mettler TA3000 system equipped with a TC10A TA processor. At least four replicate runs were performed for each sample in closed, unsealed pans at a scanning speed of 20 °C/min. The first two scans were performed over a temperature range of 40–175 °C and were immediately followed by two runs from 40 to 225 °C.

CP/MAS $^{13}$C NMR spectra were obtained on Bruker CXP-200 spectrometer equipped with a Doty probe, which allowed spinning at approximately 4 kHz, shown by the absence of spinning side bands. Most spectra were recorded at a room temperature of about 28 °C, operating at a carbon frequency of 50.307 MHz. The proton rotating-frame spin–lattice relaxation time, $T_{1\rho}(^1H)$, was measured as the reciprocal of the slope of the carbon intensity as a function of the contact time. The pulse sequence used is described in detail elsewhere.[6] It consists of a $\pi/2$ proton pulse followed by a variable $^{13}$C–$^1$H contact time and acquisition with $^1$H decoupling. There was a 10-s delay between repetitions, and contact times varied between 0.25 and 60 ms.

## Results and Discussion

All of the polymers were obtained as fine powders after precipitation and drying in vacuo at 60 °C. The homopolymers were white or light beige, whereas the copolymers were bright orange, due to the formation of a charge-transfer complex between the donor and acceptor moieties. Copolymer compositions obtained by $^1$H NMR, together with feed compositions and extents of conversion, allowed the determination of reactivity ratios at high conversions in toluene by the Kelen–Tudos method.[11] Conversions varied between 69 and 92%. Calculated reactivity ratios were $r_1 = 0.80$ for NECMM and $r_2 = 0.81$ for DNBEM. This is qualitatively similar to the values of $r_1 = 0.71$ and $r_2 = 0.55$ obtained previously in dioxane[12] in that both monomers show a slight preference for addition to the comonomer. Preliminary GPC analysis indicates peak molecular weights greater than 30 000.

The glass transition temperatures for samples prepared by different methods are given in Table I. The reported values are midpoints of the transition observed by DSC. First-run values were discarded, and the reported $T_g$ values were reproducible over three runs. Table II lists the polymers' $T_{1\rho}(^1H)$ values. Relaxation time values were obtained by taking the inverse of the slope of a semilog plot of the decay of carbon magnetization at long contact times. At least five signals were sampled: two from donor resonances free of acceptor resonance overlap, two corresponding resonances from the acceptor, and one peak at a frequency where both donor and acceptor units resonate. Figure 1 shows the spectrum of a copolymer containing 49.5 mol % NECMM, and Figure 2 indicates which carbons are responsible for these resonances, D1 and D2 for the donor (NECMM) and A1 and A2 for the acceptor (DNBEM). Since samples with different processing histories behaved differently, they will be discussed separately below.

**Table II**
**Proton $T_{1\rho}$ from CP/MAS $^{13}$C NMR**

| NECMM in copolymer, mol % | $T_{1\rho}(^1H)$, ms | | | |
|---|---|---|---|---|
| | precipitd | evapd (THF) dried 60 °C (D2) | evapd (THF) THF | evapd (THF) dried above $T_g$ |
| 0 | 25 | 20 | | |
| 13.5 | 23 | | | |
| 27.4 | 23 | 17 (15) | 15 | 24 |
| 37.1 | 23 | 20 (17) | 17 | 24 |
| 49.5 | 24 | 29 (22) | 22 | 25 |
| 62.2 | 31 | 24 (20) | 20 | |
| 73.6 | 34 | 20 | 20 | 32 |
| 87.3 | 41 | | | |
| 100.0 | 59 | 32 | | |

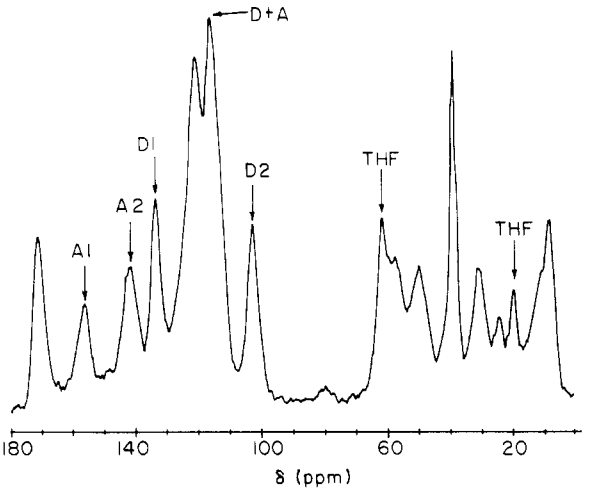


**Figure 1.** CP/MAS $^{13}$C spectrum of NECMM-*co*-DNBEM containing 49.5 mol % NECMM. Arrows indicate peaks used for $T_{1\rho}(^1H)$ calculations. This sample was prepared by slow evaporation of THF and dried at 60 °C under vacuum.

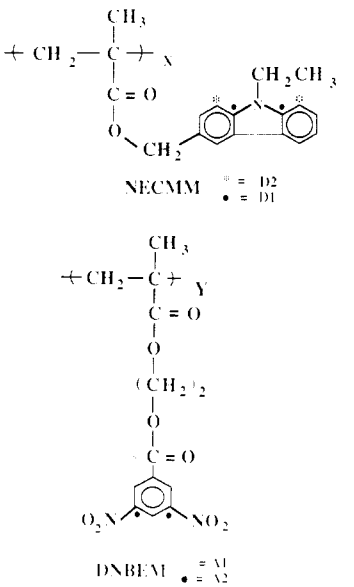


**Figure 2.** Donor (NECMM) and acceptor (DNBEM) repeat units. A1, A2, D1, and D2 are $^{13}$C resonances sampled for proton $T_{1\rho}$.

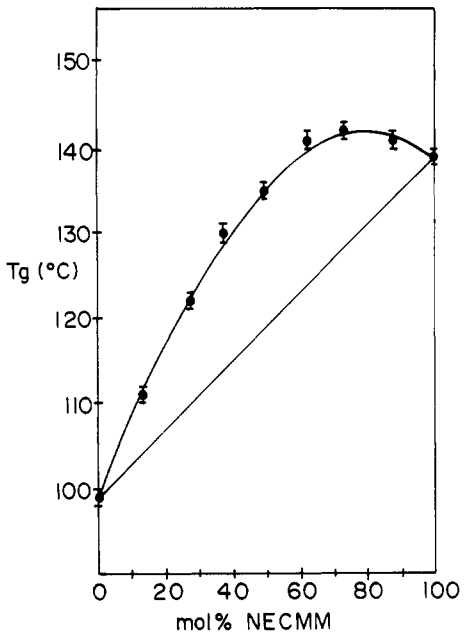


**Figure 3.** $T_g$ (°C) versus copolymer composition for precipitated samples. The solid curve represents $T_g$ calculated with the Kwei equation.

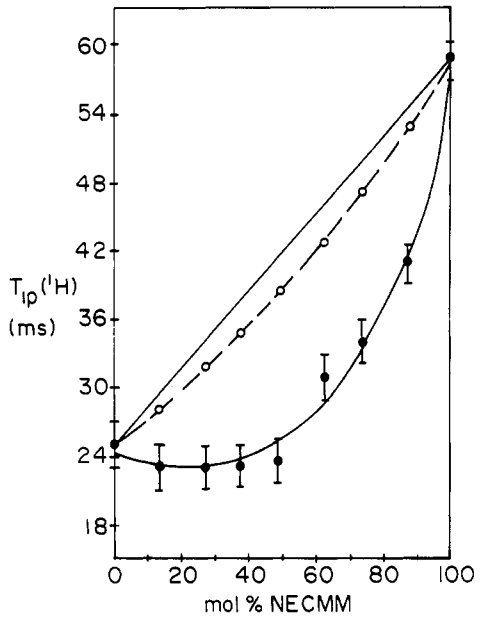


**Figure 4.** Proton $T_{1\rho}$ versus copolymer composition for precipitated samples. The dashed line and O represent values calculated with eq 4; ● are experimental points.

**Precipitated (PPTD) Samples.** The samples dried under vacuum at 60 °C after precipitation were fine, extremely static powders. A solvent evaporation peak was sometimes observed in the first run of the thermal analysis as the polymer reached its glass transition. Subsequent runs showed no traces of solvent and yielded reproducible $T_g$s. No decomplexation endotherm was observed for the precipitated samples. Drying the precipitated samples above their $T_g$s did not change the observed properties.

Figure 3 shows the variation of $T_g$ with copolymer composition. The $T_g$ values show a clear positive deviation from the weighted average of the homopolymer compositions. This deviation is thought to reflect strong inter- and intramolecular interactions, which reduce the mobility of the chains and so increase the $T_g$ above the weighted average of the homopolymers. The fitting of $T_g$ versus composition data has been attempted in many different ways. One approach has been to relate the observed $T_g$ to the fraction of various diad sequences in the copolymer. Predicted fractions of like and unlike diads can be obtained since reactivity ratios and copolymer compositions were determined. Barton[13] proposed the following equation based on the Gibbs–DiMarzio theory:

$$T_g = n_{11}T_{g11} + n_{12}T_{g12} + n_{22}T_{g22} \quad (1)$$

Johnston, on the other hand, begins with the Fox equation to give[14]

$$1/T_g = n_{11}/T_{g11} + n_{12}/T_{g12} + n_{22}/T_{g22} \quad (2)$$

Couchman[15] has proposed more complex equations that take into account the change in $\Delta C_p$ at $T_g$ for the like and unlike diads. If one ignores the change in $\Delta C_p$, then his equations reduce to the Barton or Johnston expressions.

In any event, all of the above analyses require information about the purely alternating copolymer, which was not available for this work. It is, nevertheless, instructive to work backward from the calculated diad fractions and the homopolymer $T_g$s to obtain a value of $T_{g12}$, which can fit the observed copolymer $T_g$s. The Barton equation yields an average value of 149 °C for the $T_g$ of an unlike diad, while the Johnston analysis gives 160 °C. Both seem to fit the data quite well, and without speculating on the origin of the discrepancy between the two calculated $T_{g12}$ values, it is clear that both are much higher than either homopolymer $T_g$, reflecting strong interactions between unlike repeat units due to the charge-transfer complexation.

Kwei has proposed an equation based on the Gordon–Taylor expression, which takes into account the interactions between polymers in the calculation of the $T_g$ of polymer blends:[16]

$$T_g = \frac{w_1T_{g1} + kw_2T_{g2}}{w_1 + kw_2} + qw_1w_2 \quad (3)$$

This equation only requires a knowledge of the homopolymer $T_g$s and weight fractions to define the interaction parameter, $q$. It has been shown to model well the observed $T_g$s of blends of NECMM and DNBEM homopolymers,[3] so it seems appropriate to attempt to use it for the present copolymers. Because no inflection point is observed in the plot of copolymer $T_g$ vs composition, $k = 1$. Figure 3 shows that the Kwei equation is able to fit the copolymer data well. The average value of $q$ was calculated to be 69.4, compared to the published value of 60.0 for the blends.[3] At present, our interpretation of the higher interaction parameter in the copolymers is that it reflects both inter- and intramolecular interactions, whereas only intermolecular interactions are present in the blend systems.

A discussion of the solid-state CP/MAS NMR data follows. It should be noted that preliminary studies of a small number of pNECMM/pDNBEM blends show the same trends in proton rotating-frame spin–lattice relaxation as those described herein for the copolymers. For the copolymers, an identical relaxation time was obtained for all of the resonances measured in the precipitated samples. This is a natural consequence of spin diffusion due to the abundant protons, which is expected to average the proton relaxation over the entire molecule.

Figure 4 shows the variation of $T_{1\rho}(^1H)$ with copolymer composition. In contrast to the positive deviation observed for the $T_g$ values, it is clear that the copolymers exhibit a strong negative deviation in $T_{1\rho}(^1H)$ with respect to the weighted average of the homopolymers. The shorter relaxation time is indicative of more efficient spin diffusion in the copolymers as a result of the decrease in mobility

ensuing from the interactions between the pendant donor and acceptor groups. This results in a larger component of motion at the frequency of the spin-lock field, 70 kHz in this case, which samples very slow motions. It also may imply that the attractive interactions have pulled the chains together, resulting in a smaller proton–proton distance in the blends, reducing the relaxation time and the diffusive path length. A change in spatial proximity of the protons is expected to have a dramatic effect on spin diffusion, since its efficiency varies as the inverse sixth power of the internuclear distance.[17]

Dickinson and co-workers proposed a simple linear model for the relaxation of a given component in a blend, which is dependent on the number of protons it contains[7,8]

$$1/T_{1\rho ab}(^1H) = N_aM_a/N_{total}T_{1\rho a}(^1H) + N_bM_b/N_{total}T_{1\rho b}(^1H) \quad (4)$$

where a and b are the two components of the blend ab, $M_i$ is the mole fraction of component $i$, $N_i$ is the number of protons in component $i$, and $N_{total} = M_aN_a + M_bN_b$. Figure 4 shows the predicted $T_{1\rho}(^1H)$ values for our copolymers. Clearly, this model does not describe our copolymer system adequately. This is not really that surprising, since upon blending or copolymerizing a system containing interacting units, one is bound to change the nature and correlation times of the motion, as well as the interproton distances. Therefore, the result is actually a totally new system and would not be expected to act simply as an average of its components.

It is clear from the preceding results that both DSC and proton spin diffusion show the effects of the charge-transfer interactions between the donor and acceptor units in the NECMM-*co*-DNBEM polymer. Since thermal history is well-known to affect the morphology and properties of polymers and their blends, we carried out a parallel set of experiments on a set of copolymers prepared by another method: slow evaporation of a common solvent from a dilute solution of the copolymer.

**Slow Evaporated Samples Dried at 60 °C (SE) or above the Copolymer $T_g$ (SE-TG).** Initially, we believed that it would be interesting to study slow evaporated samples because this extra processing step might allow the system to approach equilibrium more nearly than the precipitated samples. It was thought that perhaps there would be more opportunity for intermolecular interactions to take place than in samples that had essentially been frozen by fast precipitation into the state they preferred in dilute solution. One set was subjected to the same drying conditions as the precipitated samples, while the other was dried above the copolymer $T_g$.

$T_g$ values for copolymers slow evaporated from THF are also given in Table I. Figure 5 shows the effect of drying the sample at 60 °C or above $T_g$. For the samples dried only at 60 °C, there was a large solvent peak in the first run of the DSC, which occurred about 20 °C above the glass transition, not during the glass transition as in the precipitated samples. The amounts of solvent present were not determined. Sometimes several runs were needed before a reproducible $T_g$ could be obtained. Even this $T_g$ was far below that of the precipitated samples. Upon drying above $T_g$, no solvent peak was present, even in the first heating run, and the $T_g$ observed in the first run did not change in subsequent runs.

Up to this point, the behavior of the system appeared to be easy to explain. It seemed that, after drying at 60 °C, there was residual THF in the copolymers, which could not be removed because it was trapped due to the immobility of the chains. The THF would act as a small-molecule plasticizer and decrease the $T_g$. Drying above $T_g$ allowed the THF to escape, and the glass transition behavior returned almost (but not completely for some samples) to that observed for the precipitated copolymers. The solid-state NMR results we obtained were, therefore, unexpected.

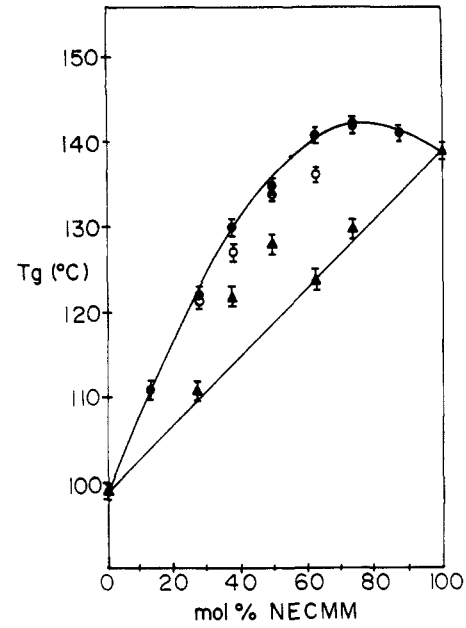


**Figure 5.** $T_g$ versus copolymer composition for different processing regimes: (●) precipitated, (▲) evaporated (THF), dried 60 °C, (○) evaporated, dried above $T_g$.

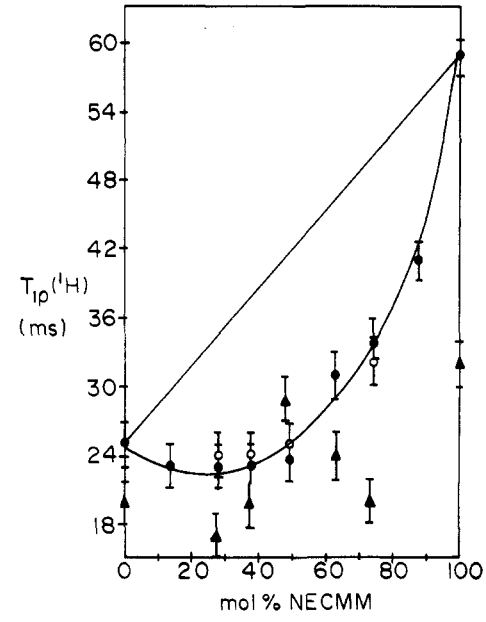


**Figure 6.** Proton $T_{1\rho}$ versus copolymer composition for different processing regimes: (●) precipitated, (▲) evaporated (THF), dried 60 °C, (○) evaporated, dried above $T_g$.

Table II lists the $T_{1\rho}(^1H)$ values for the samples prepared by slow evaporation and precipitation. Figure 6 shows graphically the relative values. In addition to the change in relaxation behavior, two additional peaks were observed in the CP/MAS $^{13}C$ spectra of the slow-evaporated copolymers dried at 60 °C at 20 and 62 ppm. From literature values of chemical shifts, it is clear that these signals are from the residual THF, which resonates at 25 and 67 ppm in the liquid state. The shift of 5 ppm upfield for these signals in the solid state indicates increased shielding, the origin of which will become apparent in the following discussion. The detection of THF in the

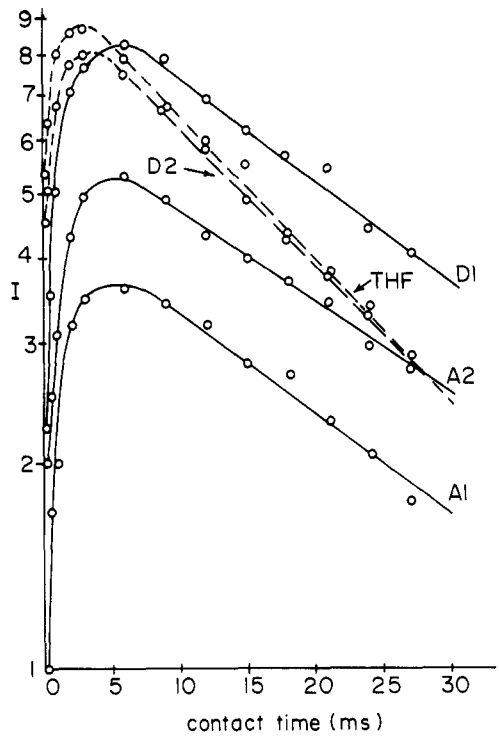


**Figure 7.** $^{13}C$ magnetization decay vs contact time (ms) for the labeled resonances.

copolymer samples was significant not only because it indicates that there are more than trace amounts present but also because it implies that the THF is not as mobile as one would expect for a plasticizer. In fact, the THF would have to be extremely tightly bound in order to generate any signal by cross-polarization, since any motion would average out the dipole–dipole interactions necessary for the application of this technique.

The influence of the bound THF is also apparent in the relaxation behavior of these samples. Not all of the peaks sampled showed the same rate of decay of the carbon magnetization. From Figure 7 it is clear that the D2 peak, which samples carbons 1 and 8 of the NECMM, decays much more quickly than the other peaks sampled. The two THF peaks were also measured as a function of time, and it was found that the $T_{1\rho}(^1H)$ of the bound solvent was identical with that obtained from the D2 peak, as Figure 7 shows. The D2 relaxation time is given in parentheses in the SE column of Table II.

From Figure 5 it can be seen that the bound THF greatly improves spin diffusion in most copolymers. More careful analysis indicates that the reduction in $T_{1\rho}(^1H)$ increases as one moves away in either direction from the 1:1 mole ratio of NECMM to DNBEM in the copolymers. Our proposed interpretation of this phenomenon involves the complexation of THF, which is known to be a good electron donor, with the acceptor unit DNBEM, in the orientation shown in Figure 8. (The aromatic shielding associated with this orientation may generate the upfield shift of the THF resonances noted earlier.) This might bring the protons on the THF ring very close to the 1,8 protons of the NECMM unit, resulting in exceedingly fast spin diffusion at this site. The trend in this effect with composition may possibly be explained by proposing that it operates between donor and acceptor groups on different chains as the concentration of copolymer increases during evaporation of the THF. Therefore, in the 1:1 copolymer, where many of the groups are complexed by intramolecular association, no increase in spin diffusion is seen. But in copolymers containing uncomplexed groups, the THF is bound and

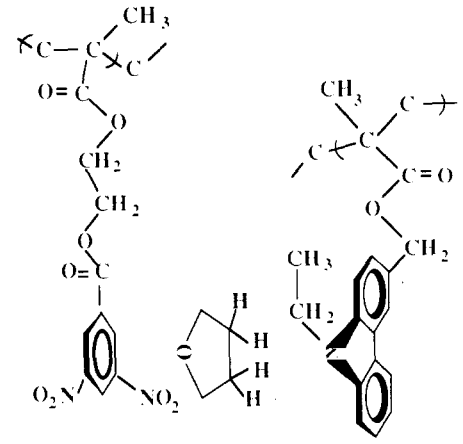

**Figure 8.** Proposed DNBEM–THF–NECMM complex.

acts as a nonbonded cross-link. It can then act to improve spin diffusion by reducing the polymer mobility and bringing a larger fraction of the motion into the very slow range to which $T_{1\rho}$ is sensitive or by providing protons in close proximity to those in the copolymer. It should be noted that the samples were subjected to identical drying conditions, but no other attempt was made to control the quantity of THF present.

The DSC data and the NMR relaxation data appear to be contradicatory as far as the effect of residual THF is concerned. A decrease in $T_g$ is usually interpreted as evidence of increased mobility, whereas more efficient spin diffusion at this low frequency implies reduced mobility and better packing resulting in shorter interproton distances. Kwei has encountered a related situation in the study of phase structure in polymer blends unrelated to NMR phenomena.[18] He explains his results as follows: in a blend of polymers having side chains that interact, the main chains may be less well packed after ordering of the pendant groups. This would cause a lowering of the energy barriers in the backbone for which the interaction of the side chains cannot compensate. If accurate, this situation could result in the behavior we observe.

The slow-evaporated copolymers dried above their $T_g$ (SE-TG) show the same behavior as all the precipitated samples, with a few exceptions that do not quite reach the $T_g$ expected, even after several DSC runs. In seems to be extremely difficult to remove the last traces of THF in some cases. No THF could be detected by DSC or by NMR, and all peaks decay at the same rate, so the residual amount must be very small.

## Conclusions

In this paper we have shown that proton rotating-frame spin–lattice relaxation time constants are useful in the study of interactions in polymers. They have also provided information about the state of residual solvent, if present. Different rates of relaxation have been observed within a system connected by covalent bonds.

Work is presently underway to compare the properties of the corresponding blends to that of the copolymers described in this work. The investigation of the copolymer properties is continuing. In addition to seeking conditions under which decomplexation can be observed in the copolymers, $T_{1\rho}(^{13}C)$ is being measured to acquire site-specific information about the complexation process in the solid state. It is hoped that variable-temperature CP/MAS NMR will also shed light on the influence of charge-transfer interactions on mobility.

**Acknowledgment.** We thank the Natural Science and Engineering Research Council of Canada and the On-

tario Centre for Materials Research for financial support. We also express our gratitude to Professor B. K. Hunter for his invaluable assistance.

## References and Notes

(1) Pugh, C.; Percec, V. *Macromolecules* **1986**, *19*, 65.
(2) Stolka, M. *Encyclopedia of Polymer Science and Engineering*; John Wiley & Sons: New York, 1988; Vol. 11, pp 154–75.
(3) Rodriguez-Parada, J. M.; Percec, V. *Macromolecules* **1986**, *19*, 55.
(4) Natansohn, A. *J. Polym. Sci., Polym. Chem. Ed.* **1984**, *22*, 3161.
(5) Natansohn, A.; Simmons, A. *Macromolecules* **1989**, *22*, 4426.
(6) Stejskal, E. O.; Schaefer, J.; Sefcik, M. D.; McKay, R. A. *Macromolecules* **1981**, *14*, 275.
(7) McBrierty, V. J.; Douglass, C. *Macromol. Rev.* **1981**, *16*, 295.
(8) Dickinson, L. C.; Yang, H.; Chu, C. W.; Stein, R. S.; Chien, J. C. W. *Macromolecules* **1987**, *20*, 1757.
(9) Simionescu, C. I.; Percec, V. *J. Polym. Sci., Polym. Chem. Ed.* **1979**, *17*, 2287.
(10) Simionescu, C. I.; Percec, V.; Natansohn, A. *Polym. Bull.* **1980**, *3*, 535.
(11) Tudos, F.; Kelen, T.; Foldes-Berezsnich, T.; Turcsanyi, B. J. *Macromol. Sci. Chem.* **1976**, *A10*, 1513.
(12) Percec, V.; Natansohn, A.; Simionescu, C. I. *Polym. Bull.* **1981**, *4*, 255.
(13) Barton, J. M. *J. Polym. Sci., Polym. Symp.* **1970**, *30*, 573.
(14) Johnston, N. W. *J. Macromol. Sci., Rev. Macromol. Chem.* **1976**, *C14*, 215.
(15) Couchman, P. R. *Macromolecules* **1982**, *15*, 770.
(16) Kwei, T. K. *J. Polym. Sci., Polym. Lett. Ed.* **1984**, *22*, 307.
(17) Caravatti, P.; Neuenschwander, P.; Ernst, R. R. *Macromolecules* **1986**, *19*, 1889.
(18) Lin, A. A.; Kwei, T. K.; Reiser, A. *Macromolecules* **1989**, *22*, 4112.
(19) Klein Douwel, C. H.; Maas, W. E. J. R.; Veeman, W. S.; Werumeus Buning, G. H.; Vankan, J. M. J. *Macromolecules* **1990**, *23*, 406.